J Electroceram (2006) 17:165–168
DOI 10.1007/s10832-006-7062-1

Conduction mechanism of grain oriented $Bi_{3.15}Nd_{0.85}Ti_3O_{12}$ ceramics fabricated by a hot-forging method

Hai Joon Lee · Chang Won Ahn · Sun Hee Kang · Sun Young Lee · Ill Won Kim · Mun Seok Choi · Jae Shin Lee · Byung Moon Jin

Received: 4 July 2005 / Revised: 5 January 2006 / Accepted: 10 January 2006

Abstract We have fabricated ordinary fired (OF) and grain oriented $Bi_{3.15}Nd_{0.85}Ti_3O_{12}$ (HF[⊥], HF[//]) samples by a hot-forging technique. The grain orientation factor F calculated from X-ray diffraction patterns of the c-axis oriented $Bi_{3.15}Nd_{0.85}Ti_3O_{12}$-HF[//] sample is determined to be above 90%. The dielectric and ferroelectric properties of $Bi_{3.15}Nd_{0.85}Ti_3O_{12}$ ceramics with different grain orientation have been investigated as a function of temperature. The a-b axis oriented $Bi_{3.15}Nd_{0.85}Ti_3O_{12}$-HF[⊥] sample had an enhanced dielectric constant (1163 at T_c) and ferroelectric properties ($P_r \sim 32\ \mu C/cm^2$). The electrical conductivity of BNT ceramic has been studied as a function of temperature in order to investigate the conduction mechanism with different grain orientations.

Keywords BNT ceramic · Grain orientation · Hot-forging · Conductivity · Dielectric constant

1 Introduction

Recently, a grain orientation technique on electro-ceramics has attracted attention for improving their electrical characteristics including ferroelectric, pyroelectric and piezoelectric properties. This technique, which is one of several ceramic preparation methods employing a controlled grain structure during the ceramic sintering process, can give the ceramics an anisotropic single crystal-like behavior. A hot-forging method seems to be the most advantageous grain orientation technique used in the laboratory for lower symmetric ceramics with a large anisotropic crystal structure, such as bismuth layered ferroelectrics [1–4]. Takenaka et al. reported that preferred grain oriented $Bi_4Ti_3O_{12}$ (BTO) ceramics fabricated by a hot-forging method improved ferroelectric and dielectric properties [1].

$Bi_4Ti_3O_{12}$, a typical material of bismuth layered ferroelectrics, is known to show large spontaneous polarization and piezoelectric constants. The polarization axis of BTO lies in the a-b plane at an angle of about 4.5° to the a-axis. Hence there is a c-axis ($P_r \sim 4\ \mu C/cm^2$) and an a-axis ($P_r \sim\ \mu C/cm^2$) component of polarization [5]. So, the thin films and ceramics of BTO suffer from high leakage current and deteriorating physical properties due to lattice defects and randomly oriented grains.

It is commonly known that proper element doping (at the Bi-site with Sm, La, Nd or Ti-site with V, Ta, Nb, W) in the perovskite-type unit of $Bi_4Ti_3O_{12}$ can effectively enhance piezoelectric and ferroelectric properties [6]. Recently, lanthanum and neodymium-substituted BTO were reported to have a relatively large remanent polarization ($2P_r \sim 24\ \mu C/cm^2$).

In this study, we have fabricated ordinary fired (OF) and grain oriented $Bi_{3.15}Nd_{0.85}Ti_3O_{12}$ (HF[⊥], HF[//]) samples by a hot-forging technique and studied the grain orientation effects on the dielectric and ferroelectric properties as well as electrical conduction behavior.

H.J. Lee · C.W. Ahn · S.H. Kang · S.Y. Lee · I. W. Kim (✉)
Department of Physics, University of Ulsan, Ulsan 680-749, Korea
e-mail: kimiw@mail.ulsan.ac.kr

M.S. Choi · J.S. Lee
School of Materials Science and Engineering, University of Ulsan, Ulsan 680-749, Korea

B.M. Jin
Department of Physics, Dong Eui University, Busan 614-714, Korea

2 Experiment

Ordinary fired $Bi_{3.15}Nd_{0.85}Ti_3O_{12}$ (BNT) ceramic samples were prepared by mixing high purity (99.9%) oxides such as Bi_2O_3, Nd_2O_3, and TiO_2 in a molar ratio with 3.15, 0.85, and 3.00, respectively, using a conventional solid state reaction method. A BNT ceramic was sintered at 1100°C for 2 hrs. Grain oriented samples were prepared by a hot-forging method (HF). Cold pressed cylindrical bodies of 17 mm in diameter and about 20 mm in height were used as starting materials for the hot forging procedure. The cylindrical bodies were sandwiched between two alumina plungers. A uniaxial pressure was statically applied along the thickness of the sample (the forging axis). The hot forged ceramics were cut from the original pellet and labeled as BNT-HF[//] and BNT-HF[⊥] in which the directions are parallel and perpendicular to the pressing axis, respectively.

The crystal structure was confirmed by X-ray diffraction (XRD) analysis, and from it the grain orientation factor, F, was calculated using the Lotgering method [7]. The Pt electrodes were formed by *dc* sputtering for electrical measurements, such as dielectric properties, ferroelectric hysteresis loops, and *dc* conductivity. The temperature dependence of the dielectric constant was measured at 1 MHz using the impedance analyzer (HP4192) in the temperature range from room temperature to 500°C. The ferroelectric *P-E* hysteresis loop was observed using a Sawyer-Tower circuit at 60 Hz. The *dc* conductivity as a function of temperature was measured using an electrometer (Keithley 237).

3 Results and discussion

Figure 1 shows the X-ray diffraction patterns of BNT samples prepared perpendicularly (HF[⊥]) and in parallel (HF[//]) to the forging axis compared with a pattern of non-oriented BNT-OF samples. XRD patterns of BNT samples exhibit a single phase of bismuth layered structure with orthorhombic symmetry. For the OF sample, the polycrystalline characteristic is shown with XRD peaks of (008), (117), and (11$\underline{1}$1). With intensities of (117) and (11$\underline{1}$1), peaks decrease and the (008), (00$\underline{1}$2) and (00$\underline{1}$4) peaks increase strongly in the HF[//] samples. In the case of HF[⊥], all the (00l) peaks disappear and (200) and (020) peaks are dominant. The grains of the OF sample are polycrystalline, but the grains of HF[//] are oriented to the *c*-axis and those of HF[⊥] are oriented to the *a-b* axis due to the applied temperature and pressure during the hot-forging process. Generally, the Lotgering factor is used to estimate the level of preferential crystallographic orientation of the grain orientation of the samples. The Lotgering's

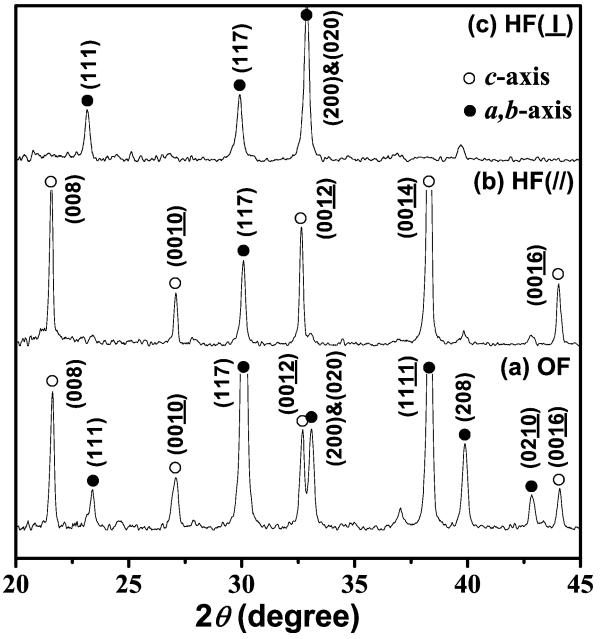

Fig. 1 XRD patterns of (a) BNT-OF, (b) HF[//] and (c) HF[⊥] samples

orientation factor (F) can be calculated using the following equation [7]:

$$P = \frac{\Sigma I(00l)}{\Sigma I(hkl)}, \quad F(\%) = \frac{P - P_0}{1 - P_0} \times 100$$

where $\Sigma I(00l)$ is the sum of the XRD intensity, reflected in the (00l) plane family and $\Sigma I(hkl)$ is the sum of the XRD intensity, reflected in all the planes. P represents the XRD patterns of the textured ceramic and P_0 can be obtained by the XRD patterns of milled powder. From the XRD analysis, the orientation factor of the HF[//] sample along the *c*-axis was $F = 90\%$.

Figure 2 shows SEM photographs obtained from (a) the BNT-OF sample and the grain oriented (b) HF[⊥] and (c) HF[//] samples. The measured surfaces were polished, and thermally etched at a sintering temperature (1100°C) for 60 min. The OF sample displays a microstructure consisting of rock-like grains and the average grain size is about 3.1 μm. It can be seen that thin plates of crystallite are piled up along the forging axis and the grains are highly oriented in the HF samples. A slip in the *c*-plane of the BNT ceramics occurs during the hot-forging process and finally the HF[//] sample is aligned to the *c*-axis, which is almost parallel to the forging axis with a well-oriented grain structure. The SEM image is consistent with the XRD results as shown in Fig. 1.

Figure 3 shows the ferroelectric *P-E* hysteresis loops for BNT-OF, HF[⊥] and HF[//] samples. The ferroelectric anisotropy of BNT is clearly observed. The remnant

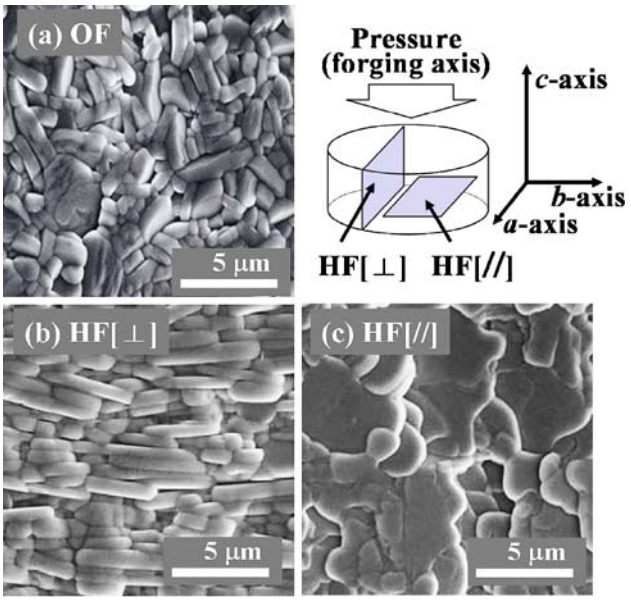

Fig. 2 SEM images of (a) BNT-OF, (b) HF[⊥] and (c) HF[//] samples

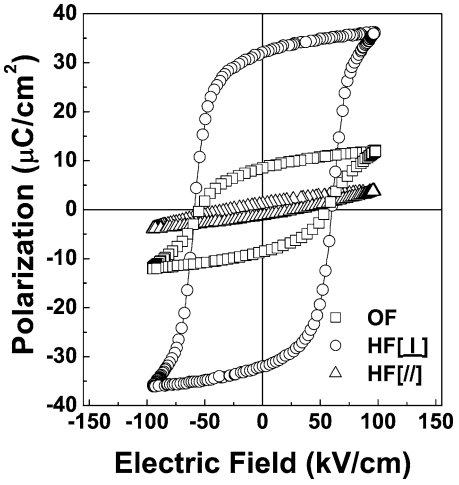

Fig. 3 Ferroelectric hysteresis loops of BNT-OF, HF[⊥] and HF[//] samples

polarization (P_r) and coercive field (E_c) of the non-oriented OF sample were 8.5 μC/cm^2 and 55 kV/cm, respectively, for the maximum applied field of 100 kV/cm, but the remnant polarization was about 4 times higher ($P_r \sim 32$ μC/cm^2) in the HF[⊥] sample, due to the grain orientation along the *a-b* axis. On the other hand, a small P_r value of 1.2 μC/cm^2 was found in the HF[//] sample, which is due to the grain orientation along the *c*-axis. The polarization axis of BNT lies in the *a-b* plane at an angle of about 4.5° to the *a*-axis. Hence, there is a *c*-axis ($P_r \sim 4$ μC/cm^2) and an *a*-axis ($P_r \sim 50$ μC/cm^2) component of polarization [5]. Our results are consistent with the result reported by Goto et al. for $Bi_{3.52}Nd_{0.48}Ti_3O_{12}$ single crystals grown along the *a-b* axis ($P_r \sim 30$ μC/cm^2) [8].

Figure 4 shows the dielectric constant of BNT-OF, HF[⊥] and HF[//] samples as a function of temperature at 1 MHz

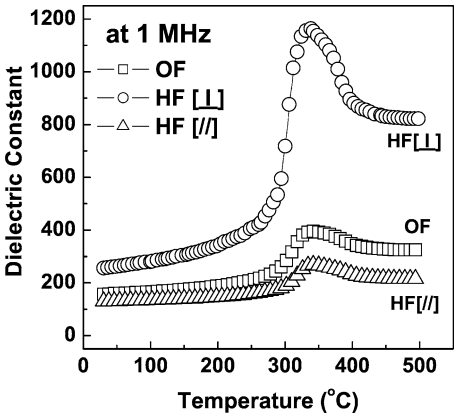

Fig. 4 Dielectric constant of BNT-OF, HF[⊥] and HF[//] samples as a function of temperature

with a fixed oscillation level voltage of 1 V. The dielectric constants of the samples increased with increasing temperature and show a maximum peak of around 340°C. The BNT HF[⊥] sample shows a typical paraelectric-ferroelectric phase transition at 340°C (Curie temperature; T_c) with a sharp dielectric constant of ∼1163, whereas the OF and HF[//] samples have a broad peak around 340°C and 342°C with a maximal dielectric constant of 395 and 268, respectively. The dielectric constants of the HF[⊥] sample were increased remarkably over the entire temperature range and the enhancement was more conspicuous around the Curie temperature compared to that of the OF sample. In contrast, the HF[//] sample has a lower dielectric constant than the OF sample. This result can be explained by the arrangement of the grains along the polarization axis (*a-b* axis) and is also consistent with the *PE* hysteresis loops as shown in Fig. 3.

Conductivity study can help to illustrate not only the effects of conductivity on the domain structure and its motion, but also the nature of charge carriers. Figure 5 shows the *dc* conductivity of BNT-OF, BNT-HF[⊥], and BNT-HF[//] samples as a function of temperature. The *dc* conductivity of the HF[⊥] sample was about one order of magnitude higher than that of the other samples in the entire temperature range [9]. The reason for the increment of *dc* conductivity for HF[⊥] is due to the anisotropic crystal structure. In the BNT structure, perovskite blocks, $[(Bi_{2-x}Nd_x)Ti_3O_{10}]^{2-}$, are interleaved with $(Bi_2O_2)^{2+}$ layers along the *c*-axis, and ferroelectricity arises mainly in the perovskite blocks along the *a-b* axis [9]. Thus, it has been reported that the resistivity along the *c*-axis is two or three orders of magnitude higher than that along the *a-b* axis because the $(Bi_2O_2)^{2+}$ layer acts as an insulating layer [10].

Different slope changes appear in different temperature regimes, indicating multiple activation processes with different energies. As the temperature increases, the space charges are released and recombined and hence, conductivities of the

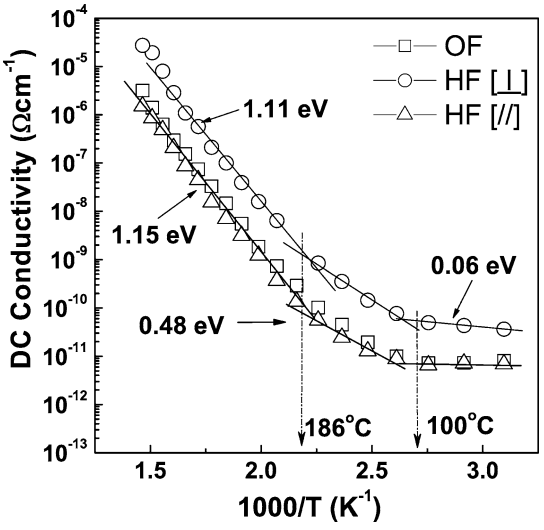

Fig. 5 DC conductivity of BNT OF, HF[⊥], and HF[//] samples as a function of temperature

samples were rapidly increased. The *dc* conductivity curves of all samples can be divided into three temperature regions. The first low temperature region is from 30°C to 100°C, the second region is up to 186°C, and the third one is above 186°C. The activation energy was calculated using the Arrhenius equation $\sigma_{dc} = \sigma_0 \exp(-E_a/k_B T)$, where k_B and E_a are the Boltzmann constant and activation energy of the electric conduction, respectively. In the low temperature region, the conductivity is almost independent of temperature and the very low value of activation energy (∼0.06 eV) corresponds to an intrinsic conduction due to the creation of a large number of space charges and other carriers [11]. The slope of *dc* conductivity in the second region was slightly increased with increasing temperature, and the activation energies (∼0.50 eV) which means that the conductivity cannot be due to any extrinsic effects and should result from the mobility of the defects and the associated charge carriers. In the high temperature region, the slopes were rapidly increased with increasing temperature, and this can be explained that the motion of oxygen vacancies in the octahedral of any perovskite structure would give rise to an activation energy (∼ 1.10 eV) [12, 13].

4 Conclusion

The grain orientation factor F of the *c*-axis oriented $Bi_{3.15}Nd_{0.85}Ti_3O_{12}$-HF[//] sample is determined to be above 90%. The *a-b* axis oriented BNT-HF[⊥] sample had an enhanced dielectric constant (1163 at T_c) and ferroelectric properties ($P_r \sim 32\ \mu C/cm^2$). The *dc* conductivity of the HF[⊥] sample ($3.64 \times 10^{-12}\ \Omega cm^{-1}$) was about one order of magnitude higher than that of other samples, because the $(Bi_2O_2)^{2+}$ layer acts as an insulating layer. In the low temperature region (30°C ∼ 100°C), the activation energy (∼0.06 eV) corresponds to an intrinsic conduction due to the creation of a large number of space charges and other carriers. In the second temperature region (100°C ∼ 186°C), the activation energies (∼ 0.50 eV) should result from the mobility of the defects and the associated charge carriers. In the high temperature region (above 186°C), the motion of oxygen vacancies in the octahedral of any perovskite structure would give rise to a high activation energy (∼ 1.10 eV).

Acknowledgments This work was supported by a Korea Research Foundation Grant (2003-002-C00065).

References

1. T. Takenaka and K. Sakata, *Jpn. J. Appl. Phys.*, **19**, 31 (1980).
2. T. Takenaka and K. Sakata, *J. Appl. Phys*., **54**, 1092 (1984).
3. M. Venet, A. Vendramini, I.A. Santos, J.A. Eiras, and D. Garcia, *Mater. Sci. Eng.,* **B117**, 254 (2005).
4. I.W. Kim, S.H. Kim, S.L. Cho, J.S. Bae, S.X. Chi, J.H. Jeong, and J.S. Lee, *Ferroelectrics*, **260**, 119 (2001).
5. S.E. Cummins and L.E. Cross, *J. Appl. Phys*., **39**, 2268 (1968).
6. H. Uchida, H. Yoshikawa, I. Okada, H. Matsuda, T. Iijima, T. Watanabe, and H. Funakubo, *Jpn. J. Appl. Phys*., **41**, 6820 (2002).
7. K. Lotgering, *Inorg. Nucl. Chem.*, **9**, 113 (1959).
8. T. Goto, Y. Noguchi, M. Soga, and M. Miyayama, *Mater. Res. Bull.*, **40**, 1044 (2005).
9. A. Rae, J. Thompson, R. Withers, and A. Willis, *Acta Crystallogr. Sect.*, **B46**, 474 (1990).
10. S.K. Kim, M. Miyayayma, and H. Yanagida, *Mater. Res. Bull.*, **31**, 121 (1996).
11. M. Mahesh Kumar and Z.G. Ye, *J. Appl. Phys*., **90**, 934 (2001).
12. W.S. Warren, K. Vanheusden, D. Dimos, G.E. Pike, and B.A. Tuttle, *J. Am. Ceram. Soc.*, **79**, 536 (1996).
13. M.J. Forbess, S. Seraji, Y. Wu, C.P. Nguyen, and G.Z. Cao, *Appl. Phys. Lett.*, **76**, 2934 (2000).